Growth, elemental analysis, thermal stability and identification of functional groups of intrinsic and manganese doped strontium tartrate pentahydrate single crystals

K.B. Reema [1,2] and N. Jagannatha [1,]*

[1] PG department of Physics, FMKMC College (A constituent college of Mangalore university), Madikeri-571201, Karnataka, India.
[2] Department of Physics, Maharani's Science College for Women (Affiliated to Mysore University), Mysuru-570005, Karnataka, India.

Email: jagannathnettar@yahoo.co.in

Abstract

Single crystals of intrinsic strontium L(+) tartrate (IST) and manganese doped strontium L(+) tartrate (MnDST) are grown by single test tube gel diffusion technique. The growth parameters are tuned to obtain an optimum condition for growth. Elemental analysis of the grown crystals is made using Energy Dispersive Analysis by X-Rays (EDAX). Fourier Transform Infrared (FTIR) and Raman techniques are used to identify various functional groups associated with the crystal lattice. Thermo Gravimetric Analysis (TGA) (in the range of 30-1030°C) is used to study the thermal stability of the grown crystals. The maximum sizes of IST and MnDST crystals of this study are 7.2×2.8×1.3 mm^3 and 3.9×1.6×1.5 mm^3, respectively. The crystals are semitransparent and yellow in color. The lattices possess various functional groups identified through their vibrational structures in FTIR and Raman spectra. Intensities of Raman peaks in the case of doped crystals are observed to be more pronounced as compared to those of IST crystals. The crystals are observed to attain thermal stability in the oxide state above 980°C. While the IST crystal is found to possess a chemical formula: $SrC_4H_4O_6.5H_2O$ with a molecular weight of 325.77, the doped MnDST crystal is found to bear a chemical formula: $Sr_{0.9883}Mn_{0.0117}C_4H_4O_6.5H_2O$ with a molecular weight of 325.38 and a cationic distribution ratio: Sr^{2+}:Mn^{2+}=84.47:1. The thermal studies also confirm the pentahydrate nature of the crystal lattices.

Keywords: *DTA, FTIR, gel technique, Raman, TGA*

1. Introduction

Gel method became operational with Liesegang's discovery of periodic crystallization in gels, an alternative technique for solution/melt growth. Among various techniques of crystal growth, gel method is relatively simple, inexpensive and convenient for growing crystals. Crystals grown by this method are sparingly soluble in water and decompose at temperature below their melting point [1, 2]. Crystals grown inside the gel are free from strain due to absence of impact of the walls of their containers [3]. Many researchers have grown intrinsic, doped and mixed tartrate crystals for specific purposes [4-8]. Tartrate crystals exhibit many interesting optical and electrical properties. Ions of transition metal- and alkaline earth- doped tartrate crystals exhibit piezoelectricity, ferroelectricity and dielectric anomalies and are useful in electronic

industries producing radio frequency controllers, ultrasonic transducers, microphones, optical and wireless communication devices.

With this background, the present work is concerned with growing manganese doped strontium L(+) tartrate pentahydrate single crystal lattice (by gel method) and to study its thermal and spectroscopic characteristics in comparison with the information on the thermal and spectroscopic characteristics of intrinsic strontium L(+) tartrate pentahydrate (already published elsewhere by the author) [9].

2. Material and Methods

Chemicals used to grow IST and MnDST crystals of this study (by gel method) are L(+) tartaric acid, strontium chloride ($SrCl_2.6H_2O$), manganese chloride ($MnCl_2.4H_2O$) and sodium meta silicate (SMS) ($Na_2SiO_3.9H_2O$). All chemicals used are of Analar grade. Gel is prepared by mixing the solution of sodium meta silicate having specific gravity ranging between 1.035-1.07 with tartaric acid of 0.5M in the ratio 5:4. The mixture is collected in glass tubes and is allowed to gel. To the set gel, chloride solutions of Sr^{2+} ions (3mL) and Sr^{2+}:Mn^{2+} ions in the ratio 5:1 are added separately and are kept undisturbed. Crystals grow in about 12 to 14 days, and are then extracted. IST and MnDST crystals are observed to have grown up to 7.2×2.8×1.3 mm^3 and 3.9×1.6×1.5 mm^3 respectively. The following chemical reactions describe the formation of IST and MnDST crystals.

$$SrCl_2.6H_2O + C_4H_6O_6 \rightarrow SrC_4H_4O_6.5H_2O + 2HCl + H_2O$$

$$MnCl_2.4H_2O + SrCl_2.6H_2O + C_4H_6O_6 \rightarrow Mn{:}Sr\ C_4H_4O_6.5H_2O + 4HCl + 4H_2O + ½O_2$$

3. Growth optimization

Optimizing the growth condition is an important aspect in growing the intended crystals successfully. A brief account of observations of this study regarding the effect of various parameters on the optimization process is made in the following subsections:

a. Effect of gel density

In the present study, growth is optimized at room temperature (23°C). For an SMS of specific gravity of 1.035, low density gel is found to form in about a week of time. Similarly, for an SMS of specific gravity 1.07, high density gel sets in smaller time duration. Denser the gel, quicker will be the setting time. High density gels are mechanically stronger than that of low density gels [10]. Denser gel is seen to result in the growth of relatively poor quality crystals as it is likely to be contaminated with silica [4]. Increase in gel density results in dendrites. Crystal count is observed to decrease with the increase of gel density. Transparency of gel is seen to be inversely related to gel density.

b. Effect of gel pH

Gel pH is observed to increase with the increase in its density. Setting of gel takes place within a few minutes for gel pH values greater than 7, where the nature of gel becomes basic. This results in dendrites. Crystal count is observed to decrease with the increase of gel pH. For pH values less than 7, the gel is acidic in nature. For gel pH between 5.1- 6.5, the gel is seen to set very quickly, and for gel pH in the range of 3.4-3.8, the gel is observed to set very slowly. In this study, good quality crystals are obtained for pH values ranging between 4.0 and 4.3.

c. Effect of gel aging

Aging of gel plays an important role in the growth of crystals [4]. Before adding the supernatant solution to the set gel of fixed pH and density, the gel is allowed to age for different periods of time. Due to gel aging, reduction in pore size and diffusivity of ions into the gel nucleation site are seen. This, in turn, reduces the crystal count.

d. Effect of concentration of supernatant

Gels of required density are prepared as described before and are allowed to set in different test tubes. In this study, supernatant having concentration in the range of 0.25-1.0 M is added to the set gel of desired pH. Both crystal count and the depth of occurrence of nucleation are seen to increase with the increase in the concentration of the supernatant.

e. Effect of quantity of upper reactant

Effect of the quantity of upper reactant on crystal count is studied by mixing SMS solution of specific gravity in the range of 1.035-1.07 and tartaric acid of 0.5 M and by allowing to age for a specific period of time. Supernatant solution varying in amount 1-5 mL is incorporated into the set gel. It is observed that, the crystal diffusion depth from the interface increases with the quantity of supernatant liquid, and the nucleation count is proportional to the quantity of upper reactant.

Based on the above observations, the growth conditions for the crystals of this study are optimized. The optimized growth parameters for the crystals are given in Table 1. The extracted IST and MnDST crystals are shown in Fig.1.

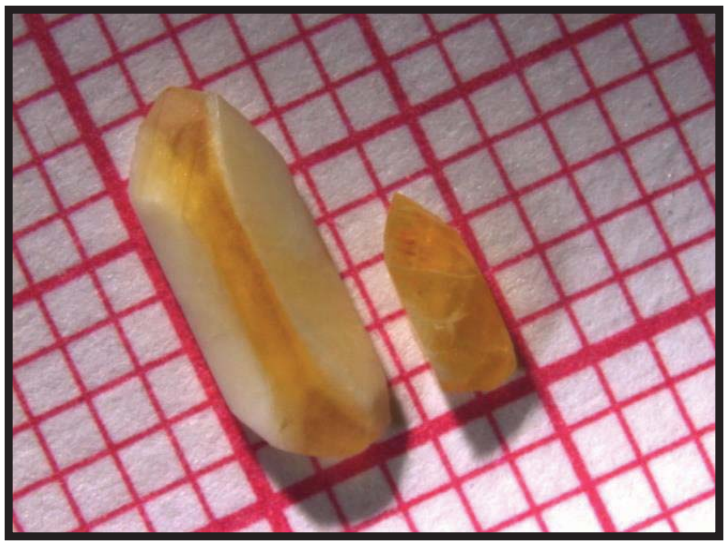

FIG 1. The extracted IST and MnDST crystals.

Table 1. Optimized growth parameters of IST and MnDST crystals.

Parameters	IST	MnDST
SMS specific gravity	1.05	1.05
Gel pH	4.00	4.00
Gel temperature (^{0}C)	23.5	23.5
SMS:Tartaric acid	5:4	5:4
Reactants ratio	-	$SrCl_2$:$MnCl_2$ = 5:1
Reactants concentration (M)	0.5	0.5
Duration of growth (days)	12	13
Color	Lemon yellow	Pale yellow
Size (l×b×h) mm^3	7.2×2.8×1.3	3.9×1.6×1.5
Morphology	Cylindrical, hard and transparent	Hillocky pyramidal, hard and transparent

4. Characterization

The harvested crystals are characterized with the help of different techniques of instrumentation and analysis. pH of gel is optimized using digital pH meter EQ-614A (QUIP-TRONIC). Incorporation of manganese and the surface morphology of the crystals are studied using CARL ZIESS FESEM (Oxford instruments) attached with EDS system [9]. Fourier transform infrared (FTIR) spectra for the powdered sample is recorded in the wave number range of 400-4000 cm^{-1} for both intrinsic and doped crystals using Bruker (Alpha) infrared spectrometer adapted KBr pellet technique. Laser Raman spectroscopic (Raman) measurements are made using Raman microscope: Horiba scientific Xplora Plus, with 532nm laser source. Thermal stability and decomposition behavior of the grown crystals are studied using TG-DTA simultaneous

thermal analyzer (NETZSCH STA 2500A-0027-N) instrument at temperatures in the range of 30-1030^{o}C, with a heating rate of 3^{o}C/min.

5. Result and discussion

a. EDAX measurement

The presence of elements in the grown crystals is identified by performing quantitative elemental analysis. Fig. 2 and Fig. 3 confirm the presence of Sr^{2+} in the crystals and Mn^{2+} ions in the MnDST lattice. EDAX spectrum for the crystals confirm the presence of elements, namely, Sr, C and O in IST and Mn, Sr, C and O in MnDST crystal lattices. The atomic and weight percentages of the constituent elements of the grown crystals are shown in Table 2. The estimated cationic distribution from the EDAX measurement of MnDST crystal is found to be: Sr^{2+}:Mn^{2+}=84.47:1. Resulted morphological change due to doping of Mn^{2+} into Sr^{2+} vacancies are seen in the SEM images, shown in Fig. 4 and Fig. 5.

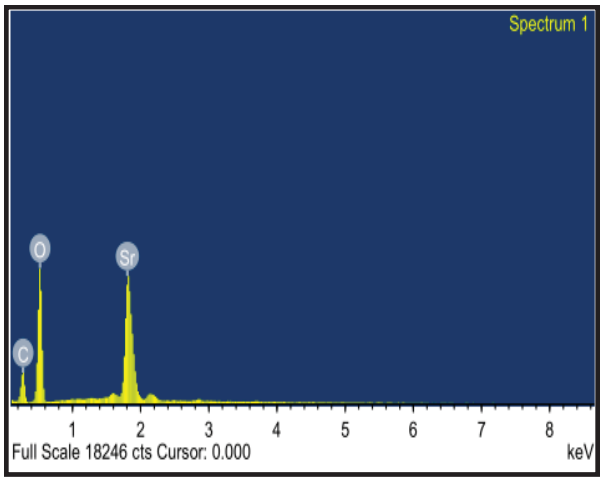

FIG 2.EDAX spectrum- IST crystal.

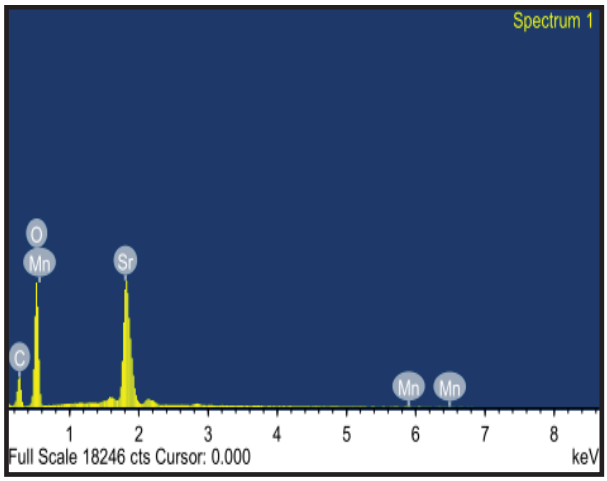

FIG 3.EDAX spectrum- MnDST crystal.

Table 2. Atomic and weight percentages of the constituent elements.

Crystal	Parameter	ELEMENTS			
		O	Mn	Sr	C
IST	Weight %	49.86	-	31.42	18.72
	Atomic %	61.92	-	07.12	30.96
MnDST	Weight %	48.65	0.25	32.80	18.30
	Atomic %	61.55	0.09	07.58	30.78

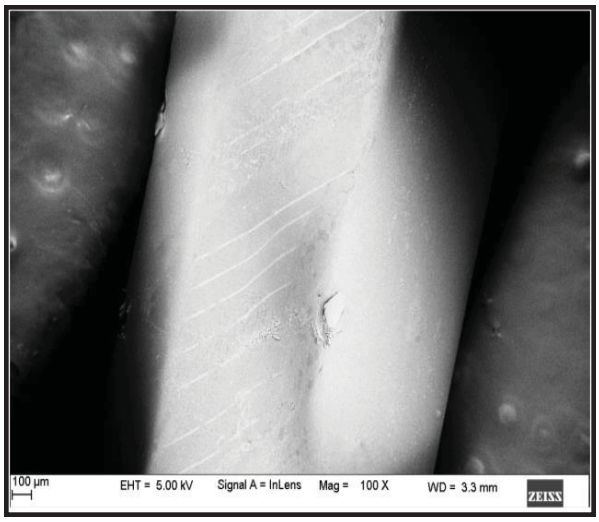

FIG 4.SEM image of IST crystal.

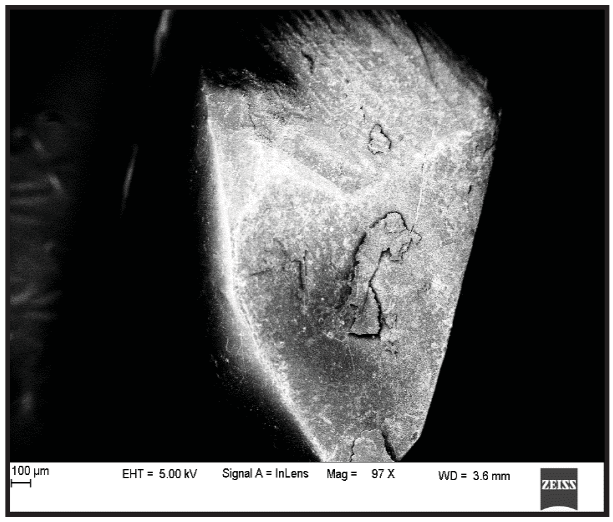

FIG 5.SEM image of MnDST crystal.

b. FTIR and Raman spectral analysis

Functional groups and the possible stretching and vibrational aspects of the grown crystals are shown in Fig. 6 and Fig. 7 respectively.

The peaks of interest to this study in these spectra are also marked in Fig. 6 and Fig. 7. Assignments for various spectral peaks are shown in Table 3. Comparison of Raman spectra in Fig. 6 (for IST) and Fig. 7 (for MnDST) reveal enhancement of characteristic Raman intensity peaks due to doping. Also evident from Fig. 6 and Fig. 7 is that the information of molecular vibrations from Raman spectra is consistent with those from FTIR for both IST and MnDST crystals.

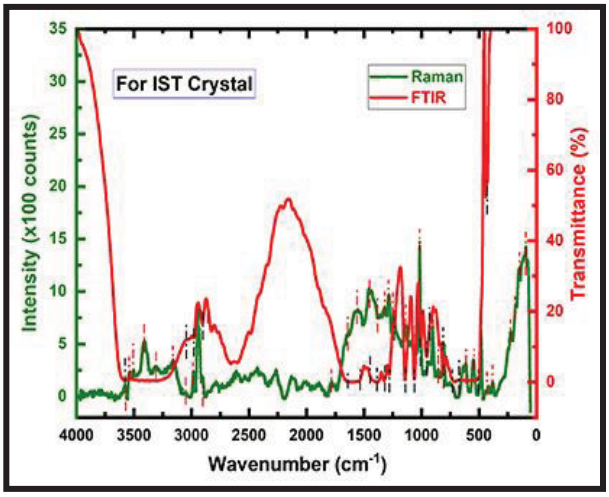

FIG 6. FTIR and Raman spectra- IST crystal.

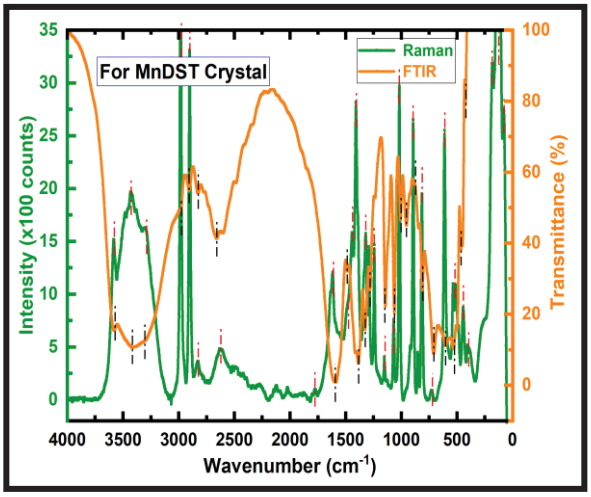

FIG 7. FTIR and Raman spectra- MnDST crystal.

Table 3. FTIR and Raman spectra for IST and MnDST crystals.

IST CRYSTALS		MnDST CRYSTALS		Assignments	References
FTIR absorption band/peaks (cm^{-1})	Raman emission band/peaks (cm^{-1})	FTIR absorption band/peaks (cm^{-1})	Raman emission band/peaks (cm^{-1})		
3580-3044	3580, 3537, 3503, 3407, 3300, 3155, 3044	3580-3290	3583, 3427, 3286	O-H stretch $\gamma_1(H_2O)$ $\gamma_3(H_2O)$	[11, 12]
2981, 2903	2981,2947 and 2903	2980, 2905 2829	2980, 2905, 2829	C-H stretch	[12-18]
-	1780	-	1780	C=O stretch	[11, 14, 18, 19]
1650	1650	1599	1614	$\gamma_2(H_2O)$	[12]
1557	1557	1552, 1485	1552, 1480	COO^- Asymmetric stretch	[12-14], [16], [20]
1455	1455	1443	1447	COO^- symmetric stretch	[12-14], [16], [20]
1393	1393, 1359	1388	1409	O-H bending and deformation	[12-14], [16]
1320, 1277 and 1233	1325, 1277 and 1233	1330, 1281, -	1324, 1291, 1249	C-H bend	[12-14]
1141, 1060	1136, 1078	1141, 1065	1152, 1065	C-O symmetric stretch	[11-14]
1005, 953, 904	1005, 942, 904	1007, 958, 878	1012, - , 894	C-C symmetric stretch	[2, 16, 20, 21]
812, 610	803, 610	812, 711, 609	812, 727, 609	COO^- deformation	[12, 14]
546, 488, 436	546, 488, 436	522, 431	522, 442	Metal- Oxygen bond	
-	382, 226, 190, 151, 92	-	399, 184, 130	Skeletal deformation COO^- twist and C-C torsion	[12-14]

5.3 Thermal studies

TG-DTA plots for IST and MnDST crystals are shown in Fig. 8 and Fig. 9, respectively, for a temperature range of 30-1030^{o}C. The process of decomposition of IST and MnDST lattice may be briefly accounted as follows: In Fig. 8, the first stage of decomposition of IST crystal occurs in the range of 73 - 190^{o}C. In this stage, the crystal undergoes a weight loss of 17.05% (calc. loss 16.59%) with the elimination of 3 water molecules. This corresponds to the endothermic peaks at 136^{o}C and 172^{o}C. In the second stage of decomposition occurring in the range of 190-335^{o}C, the crystal suffers a loss of weight of 19.59% (calculated loss 20.27%). This is due to the elimination of two coordinated water molecules and liberation of formaldehyde gas [22], confirmed by the simultaneous endothermic (262^{o}C) and exothermic (279^{o}C) peaks. During the third stage of decomposition (in the range of 335-470^{0}C), the crystal suffers a weight loss of 14.09% (calculated loss 14.13%) with the elimination of a molecule of water (evidenced by the endothermic peak at 386^{o}C) and liberation of carbon monoxide (evident from the exothermic peak at 415^{0}C). In the fourth and final stage of decomposition (in the range of 836-1000^{0}C), the crystal reduces to strontium oxide with the liberation of two molecules of carbon monoxide [22].

In the first stage of decomposition of MnDST lattice (Fig. 9) occurring in the range 61-150^{o}C, the crystal suffers a weight loss of 17.55% (calculated loss: 16.61%). This is due to the elimination of 3 water molecules, supported by the endothermic peaks at 47.3^{o}C and 137^{o}C. In the second stage of decomposition (in the range of 150-306^{o}C), the crystal suffers a weight loss of 21.34% (calculated loss 20.30%). This is attributed to an elimination of two coordinated water molecules with the liberation of formaldehyde gas [22], confirmed by the simultaneous endothermic (270^{o}C) and exothermic (285^{o}C) peaks. The third stage of decomposition, occurring between 306 and 717^{o}C, corresponds to a weight loss of 14.23% (calculated weight loss: 14.14%). This weight loss is due to elimination of a molecule of water (supported by the endothermic peak at 669 ^{o}C) along with the liberation of carbon monoxide (evidenced by the exothermic peak at 448^{o}C). Fourth and final stage of decomposition, identified in the range of 717-1030^{o}C, is accompanied by a weight loss of 15.77% (Calculated loss 17.22%). As a result, the crystal attains stability as strontium manganese oxide with the liberation of two molecules of carbon monoxide [22].

From the above analysis, it is clear that, in the process of attaining thermal stability, both the grown crystal lattices lose five water molecules before reaching stability. This indicates the presence of five water molecules in the grown crystal lattices.

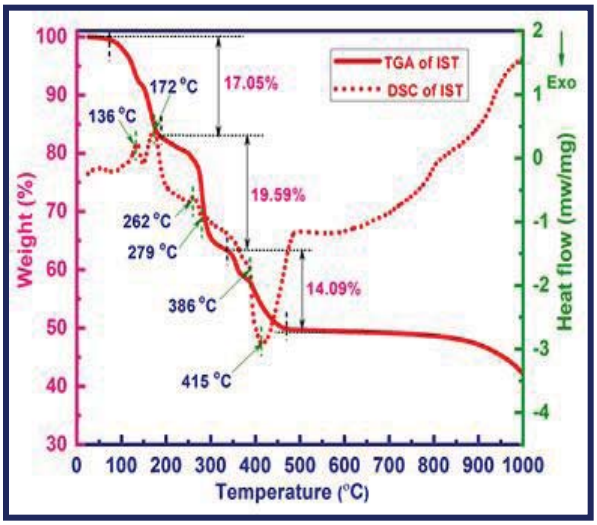

FIG 8.TG plot of IST crystal

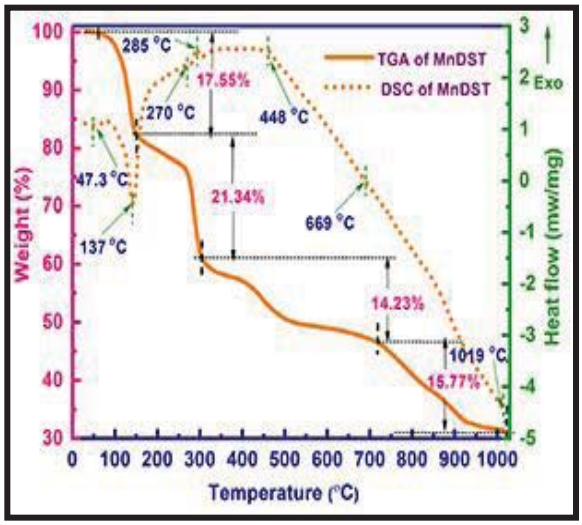

FIG 9.TG plot of MnDST crystal

Table 4. Decomposition process of IST and MnDST crystals.

Crystals	Decomp. stage	Temp. range (°C)	Observed weight loss (%)	Theoretical weight loss (%)	Reactions
IST	I	73 - 190	17.05	16.59	$SrC_4H_4O_6.5H_2O \rightarrow SrC_4H_4O_6.2H_2O + 3H_2O$
	II	190 - 335	19.59	20.27	$SrC_4H_4O_6.2H_2O \rightarrow SrC_3H_2O_5 + 2H_2O + H_2CO$
	III	335 - 470	14.09	14.13	$SrC_3H_2O_5 \rightarrow SrC_2O_3 + H_2O + CO$
	IV	836-1000	-	-	$SrC_2O_3 \rightarrow SrO + 2CO$
MnDST	I	61-150	17.55	16.61	$Sr_{0.9883}Mn_{0.0117}C_4H_4O_6.5H_2O \rightarrow Sr_{0.9883}Mn_{0.0117}C_4H_4O_6.2H_2O + 3H_2O$
	II	150 - 306	21.34	20.30	$Sr_{0.9883}Mn_{0.0117}C_4H_4O_6.2H_2O \rightarrow Sr_{0.9883}Mn_{0.0117}C_3H_2O_5 + 2H_2O + H_2CO$
	III	306 - 717	14.23	14.14	$Sr_{0.9883}Mn_{0.0117}C_3H_2O_5 \rightarrow Sr_{0.9883}Mn_{0.0117}C_2O_3 + H_2O + CO$
	IV	717 - 1030	15.77	17.22	$Sr_{0.9883}Mn_{0.0117}C_2O_3 \rightarrow Sr_{0.9883}Mn_{0.0117}O + 2CO$

Table 5. DTA profile of IST and MnDST crystals.

IST		MnDST	
Reaction	DTA Peak temperature (^oC)	Reaction	DTA Peak temperature (^oC)
Endo	136, 172	Endo	47.3, 137
Endo, Exo	262, 279	Endo, Exo	270, 285
Endo, Exo	386, 415	Exo, Endo	448, 669

6. Conclusion

Intrinsic strontium L(+) tartrate (IST) and manganese doped strontium L(+) tartrate (MnDST) crystals are grown by gel method under optimized growth conditions. These crystals are characterized by various techniques (EDAX, FTIR, Raman and TG-DTA) to study their elemental, ionic and thermal nature. The IST crystals appear to possess a chemical formula: $SrC_4H_4O_6.5H_2O$ with a molecular weight of 325.77 and the doped MnDST crystal is found to have a chemical formula: $Sr_{0.9883}Mn_{0.0117}C_4H_4O_6.5H_2O$ with a molecular weight of 325.38 and a cationic distribution ratio: Sr^{2+}:Mn^{2+}=84.47:1. Thermal studies of the crystals confirm the penta-hydrate nature of the grown crystal lattices. The crystals are found to attain thermal stability in the oxide state, indicating usefulness of these crystals in high temperature electronics.

7. Acknowledgements

The authors are grateful to both Principal and Head of the department of Physics, FMKMC College, Madikeri for providing the infrastructure support to this research work. One of the authors (KBR) acknowledges the help and support given by the faculty members of Department of Science and Technology-Promotion of University Research and Scientific Excellence (DST-PURSE) laboratory, Mangalore University, Mangalore, Center for materials science and technology, Vijnana bhavan, University of Mysore, Mysuru and Department of chemistry, National Institute of Technology (NITK), Surathkal, Mangalore with regard to the elemental analysis (FESEM/EDS), TG-DTA, Raman and FTIR studies of the samples.

REFERENCES

[1] H.K. Hektisch, J. Dennis and J.I. Hanoka, Journal of Physics and Chemistry of Solids *26*(3), 493-496 (1965)

[2] B.S. Kumar, M.R. Kutty, M.S. Kumar and K.R. Babu, Bulletin of Materials Science 30(4), 349-355 (2007)

[3] S.S. Sonawane, S. J. Nandre, R.R. Ahire and S.J. Shitole, Der Pharma Chemica 6(3), 33-38 (2014)

[4] H.J. Nickl and H.K. Henisch, Journal of the Electrochemical Society 116(9), 1258 (1969)

[5] A.R. Patel and S.K. Arora, Journal of Materials Science 11(5), 843-846 (1976)

[6] N. Jagannatha and P.M. Rao, Bulletin of Materials Science 16(5), 365-369 (1993)

[7] K. Suryanarayana, S.M. Dharmaprakash, K. Sooryanarayana, Bulletin of Materials Science 21(1), 87-92 (1998)

[8] A.R. Patel and S. K. Arora, Journal of Crystal Growth 37(3), 343-345 (1977)

[9] K.B. Reema, N. Jagannatha, K. P. Nagaraja and D. D'Souza, JOURNAL OF ADVANCED APPLIED SCIENTIFIC RESEARCH *3*(1), 7-15 (2021)

[10] S.K. Arora, Vipul Patel, Anjana Kothari and Brijesh Amin, Crystal growth & design 4(2), 343-349 (2004)

[11] L.I. Kozhevina, L.G. Skryabina and Yu K. Tselinskii, Journal of Applied Spectroscopy *33*(6), 1347-1351 (1980)

[12] N. Kaneko, M. Kaneko and H Takahashi, Spectrochimica Acta Part A: Molecular Spectroscopy 40(1), 33-42 (1984)

[13] P. Kolandaivel and S. Selvasekarapandian, Crystal Research and Technology *28*(5), 665-670 (1993)

[14] M. Ben Salah, K. Mouaine, P. Becker and C. Carabatos-Nédelec, physica status solidi (b) *220*(2) 1025-1032 (2000)

[15] X.S Shajan and C. Mahadevan, Bulletin of Materials Science *27*(4), 327-331 (2004)

[16] H.M. Patil, D.K. Sawant, D.S. Bhavsar, J.H. Patil and K.D. Girase, Journal of thermal analysis and calorimetry *107*(3), 1031-1037 (2012)

[17] D. Lin-Vien, N.B. Colthup, W.G. Fateley and J.G. Grasselli, The handbook of infrared and Raman characteristic frequencies of organic molecules Elsevier (1991)

[18] R. Bhattacharjee, Y.S. Jain and H.D. Bist, Journal of Raman spectroscopy *20*(9), 561-567 (1989)

[19] Edsall and T. John, The Journal of Chemical Physics *5*(7), 508-517 (1937)

[20] A.V.R. Warrier and R.S. Krishnan, Spectrochimica Acta Part A: Molecular Spectroscopy 27(8), 1243-1246 (1971)

[21] A. Firdous, I. Quasim, M.M. Ahmad and P.N. Kotru, Crystal Research and Technology: Journal of Experimental and Industrial Crystallography 43(10), 1015-1021 (2008)

[22] T. Fukami, S. Tahara, C. Yasuda and K. Nakasone, International Research Journal of Pure and Applied Chemistry 1-10 (2016)